International Journal of Heat and Mass Transfer 52 (2009) 4151–4159

Contents lists available at ScienceDirect

International Journal of Heat and Mass Transfer

journal homepage: www.elsevier.com/locate/ijhmt

Monte Carlo simulation of transient radiative transfer in a medium with a variable refractive index

C.Y. Wu *

Department of Mechanical Engineering, National Cheng Kung University, Tainan 701, Taiwan, ROC

ARTICLE INFO

Article history:
Received 26 September 2008
Received in revised form 19 February 2009
Accepted 22 April 2009
Available online 6 June 2009

Keywords:
Transient radiative transfer
Monte Carlo simulation
Variable refractive index
Anisotropically scattering
Pulse irradiation

ABSTRACT

In this work, a Monte Carlo method is developed to simulate transient radiative transfer in a refractive planar medium exposed to a collimated pulse irradiation. The time of flight in closed form is derived for a medium with a linearly varying refractive index. The time-resolved reflectance and transmittance of the slab are obtained by tracing photon bundles and calculating the time of flight. There is a very satisfying correspondence between the present results and the discrete ordinates solutions. The magnitude of numerical uncertainty decreases with the increase of bundles. To simulate transient radiative transfer in an optically thick medium, we need a large number of bundles. The reflectance decreases with the increase of the positive gradient of the refractive index considered. The appearance instant of the transmittance peak postpones as the refractive index increases. Influence of the optical thickness, the scattering albedo and the anisotropically scattering coefficient on the time-resolved reflectance and transmittance is also investigated.

1. Introduction

Interest in the radiative transfer problems incorporating the spatially continuous variation of refractive index is obtaining more attention in the last decade. The radiative energy transfers in curved paths rather than straight lines and the propagation speed of the energy is a function of the position due to the continuous variation of refractive index. The complicated radiative transfer problems are of great importance in atmosphere, optical imaging of biological tissues and plasma diagnostics. Quasi-steady radiative heat transfer in a medium with a variable refractive index has been analyzed by many researchers with rigorous methods, such as, the curved ray-tracing technique [1–3], a combined curved ray-tracing method and pseudo source adding method [4,5], the discrete ordinates method [6,7], the Monte Carlo method [8–10], the finite element method [11], the discrete transfer method [12] and the least square spectral element method [13]. Due to the availability of short-pulse lasers, the consideration of the transient term in the radiative transfer equation is necessary. Some of the researchers derived and debated the equation for transient radiative transfer in a medium with a varying refractive index. In 1999, Ferwerda [14] derived the transient radiative transfer equation for a scattering medium with a spatially varying refractive index. Tualle and Tinet [15] developed the transient radiative transfer equation in a scattering medium with a spatially varying refractive index. They also reported the results of diffusion approximation and Monte Carlo simulation for the case with a point source. Premaratne and coworkers [16] obtained the photon transport equation for turbid biological media with spatially varying refractive index using the principle of energy conservation and laws of geometrical optics. They have showed that their result reduces to the standard radiative transfer equation when the refractive index is constant and to the geometrical optics equation when the medium is lossless and non-scattering. There are only a few rigorous solutions for transient radiative transfer in a medium varying refractive index. Except Tualle and Tinet's Monte Carlo simulation for the case with a point source [15], Wu [17] presented a discrete ordinates solution of transient radiative transfer in a refractive slab with a pulse irradiation and Liu and Hsu [18] studied transient radiative transfer in one- and two-dimensional refractive media using the discontinuous finite element method. In this work, a Monte Carlo method is developed to simulate transient radiative transfer in a slab with a linearly varying refractive index. The reasons to adopt the Monte Carlo method are that the Monte Carlo method is recognized as an accurate method and the accuracy of its prediction depends on the sample size, i.e., the number of bundles [19]. Thus, the numerical solutions obtained by the Monte Carlo method using a very large number of bundles may be considered as benchmarks. In a medium with linear distribution of refractive index, the curved ray trajectory can be expressed as an analytical explicit function [1–2]. For Monte Carlo simulations of transient radiative transfer, the path length of each curved trajectory has to be converted to time of flight by using the varying speed of light in the refractive medium. The time of flight in a medium with linear distribution of refractive index is deduced analytically in this work. The

* Tel.: +886 6 2757575 62151; fax: +886 6 2352973.
E-mail address: cywu@mail.ncku.edu.tw

0017-9310/$ - see front matter © 2009 Elsevier Ltd. All rights reserved.
doi:10.1016/j.ijheatmasstransfer.2009.04.012

Nomenclature

a_1	anisotropically scattering coefficient
c_0	speed of light in vacuum
E	energy
H	Heaviside step function
I	radiative intensity
I_P	truncated Gaussian pulse
I_0	maximum irradiation intensity
L	thickness of the slab
n	refractive index
n_0	refractive index at $z = 0$
n_S	refractive index at $z = L$
N	total number of photon bundles
R	time-resolved reflectance
R_n	random number
t	time
t_c	instant when the I_0 enters the medium
t_f	time of flight
$t_{f>}$	time of flight, Eq. (13)
t_p	FWHM of the pulse irradiation
t^*	dimensionless time
T	time-resolved transmittance
s	path length of a curved bundle trajectory
z	geometrical coordinate
z_r	location of internal reflection
Greek symbols	
β	extinction coefficient
δ	Dirac delta function
θ	polar angle
μ	$\mu = \cos\theta$
τ_L	optical thickness
Φ	scattering phase function
ω	scattering albedo

closed-form path length and time of flight are beneficial to the efficiency of the Monte Carlo simulation. After deriving the time of flight, we consider problems with a collimated pulse irradiation. The time-resolved reflectance and transmittance of the slab are obtained for various optical thicknesses, scattering albedos, anisotropically coefficients and gradients of refractive index. These results are compared with those obtained by the discrete ordinates method [17].

2. Formulation of the problem

Consider transient radiative transfer in a refractive, absorbing and anisotropically scattering slab of thickness L, as shown in Fig. 1. The boundary at $z = 0$ is exposed to pulse irradiation and is bounded by vacuum or a non-participating semi-infinite medium with refractive index $n_0 = 1$. The boundary at $z = L$ is free from irradiation and is bounded by a non-scattering semi-infinite medium with a constant refractive index $n_s > 1$.The refractive index of the medium varies linearly in the z-direction by the relationship

$$n(z) = n_0 + (n_s - n_0)z/L. \tag{1}$$

The external irradiation may be a collimated pulse irradiation expressed as

$$I(0,\mu,t) = I_p(t)\delta(\mu - 1), \quad \mu > 0, \quad t > 0, \tag{2}$$

where $I_p(t)$ is a truncated Gaussian pulse expressed as

$$I_p(t) = I_0 \exp\left[-4\ln 2\left(\frac{t-t_c}{t_p}\right)^2\right]\{H[t-(t_c-3t_p)] - H[t-(t_c+3t_p)]\} \tag{3}$$

with I_0 denoting the maximum intensity at $t = t_c$, t_p denoting the full width at half maximum (FWHM) of the pulse irradiation, H denoting the Heaviside step function and δ denoting the Dirac delta function. Here, for simplicity, we assume the emission of the medium to be negligible compared with the incident radiation and consider linearly anisotropic scattering as follows:

$$\Phi(\mu,\mu') = 1 + a_1\mu\mu', \tag{4}$$

where a_1 denotes the anisotropically scattering coefficient.

The traditional Monte Carlo method has been described in standard textbooks [19,20] in detail. Besides, the Monte Carlo simulation of transient radiative transfer in a planar medium with a constant refractive index has been reported by Jacques [21], Brewster and Yamada [22], Wu and Wu [23] and Guo and coworkers [24]. Thus, we focus on the simulation of the curved ray tracing and the calculation of the time of flight along the curved trajectory in the present work.

The initial time of the incident photon bundle in one pulse is selected by a random number generator. The path length that any bundle may travel without being absorbed or scattered can be sampled as

$$s = \frac{1}{\beta}\ln\left(\frac{1}{R_n}\right), \tag{5}$$

where β is the extinction coefficient and R_n is a random number. For the present case with linear distribution of refractive index, the path length of a curved bundle trajectory to the next absorption or scattering can be deduced from the expression given by Ben Abdallah and Le Dez [1]

$$ds(z') = \frac{n(z')}{\sqrt{n^2(z') - n^2(z_1)[1-\cos^2(\theta_1)]}}dz'. \tag{6}$$

The resulting expression of the path length in terms of z_1, θ_1 and z_2 for the trajectory shown in Fig. 1(a) is

$$s(z_1,\cos\theta_1,z_2) = \frac{L}{(n_s-n_0)}\left[\sqrt{n^2(z_2) - n^2(z_1)\sin^2\theta_1} - n(z_1)\cos\theta_1\right], \quad \theta_1 < \pi/2. \tag{7}$$

Here, the subscript 1 denotes the location inside or on the boundaries of the medium for scattering or incidence of a bundle, and the subscript 2 denotes the position where a bundle is absorbed or scattered. Solving Eq. (7), we can calculate the position of the next absorption or scattering from

$$z_2 = \frac{L}{(n_s-n_0)}\sqrt{\left[\frac{s(n_s-n_0)}{L} + n(z_1)\cos\theta_1\right]^2 + n^2(z_1)\sin^2\theta_1} - \frac{n_0 L}{(n_s-n_0)}, \quad \theta_1 < \pi/2, \tag{8}$$

where the s is determined by Eq. (5). The expression for the position of the next absorption or scattering on a curved trajectory with $\theta_1 > \pi/2$ can be deduced similarly. However, the boundary $z = 0$ cannot be reached by a bundle passing through the point z_1 with $\cos\theta_1$ between 0 and $-\sqrt{1-[n_0/n(z_1)]^2}$, as shown in Fig. 1(b). Such a bundle tends to the point

$$z_r = \frac{L}{(n_s-n_0)}[n(z_1)\sin\theta_1 - n_0] \tag{9}$$

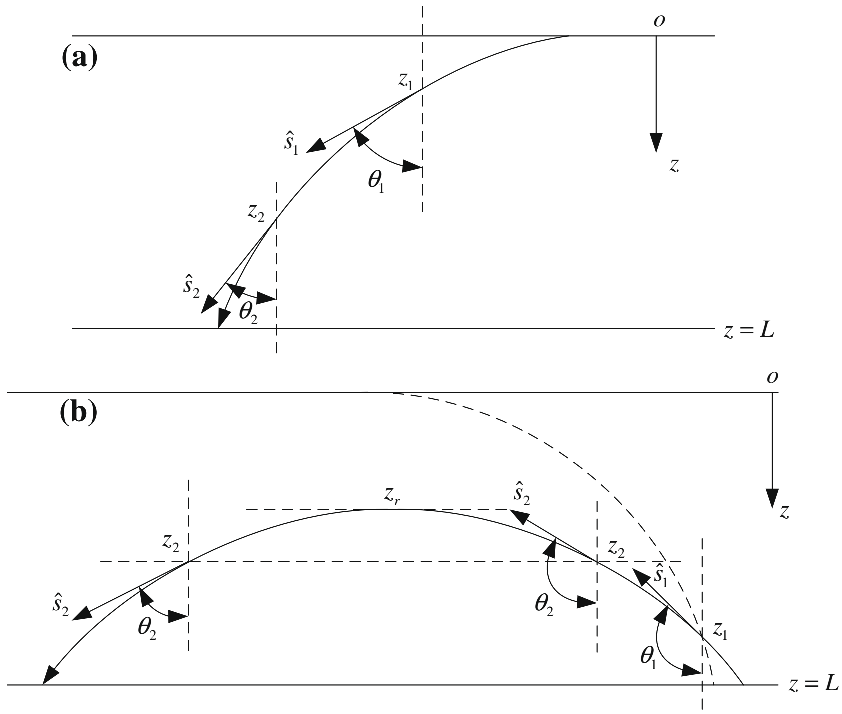

Fig. 1. Coordinates and ray tracing: (a) $\theta_1 < \pi/2$; (b) $\theta_1 > \pi/2$.

and reflects back toward the boundary $z = L$. The special trajectory with $z_r = 0$ is shown as a dash curve in Fig. 1(b).

To simulate transient radiative transfer, the path length of each curved trajectory has to be converted to the time of flight by using the varying speed of light in the refractive medium

$$\int_{t_1}^{t_2} dt(z) = \int_{z_1}^{z_2} \frac{1}{c_0 n(z')} ds(z'), \tag{10}$$

where c_0 is the speed of light in vacuum. Substituting Eqs. (1) and (6) into Eq. (10), we obtain the closed-form flight time of bundles along a curved trajectory

$$\begin{aligned} t_f(z_1,\cos\theta_1,z_2) = \frac{L}{2c_0(n_s-n_0)}\Big\{ & n(z_2)\sqrt{n^2(z_2)-n^2(z_1)\sin^2\theta_1} \\ & + n^2(z_1)\sin^2\theta_1 \ln\left[\sqrt{n^2(z_2)-n^2(z_1)\sin^2\theta_1}+n(z_2)\right] \\ & - n^2(z_1)\cos\theta_1 - n^2(z_1)\sin^2\theta_1 \ln[n(z_1)\cos\theta_1 + n(z_1)]\Big\}, \end{aligned} \tag{11}$$

which is valid for $\cos\theta_1 > 0$. Similarly, for the curved trajectory with $\cos\theta_1$ in the interval $[-1, -\sqrt{1-[n_0/n(z_1)]^2}]$, we can deduce

$$\begin{aligned} t_f(z_1,\cos\theta_1,z_2) = \frac{-L}{2c_0(n_s-n_0)}\Big\{ & n(z_2)\sqrt{n^2(z_2)-n^2(z_1)\sin^2\theta_1} \\ & + n^2(z_1)\sin^2\theta_1 \ln\left[\sqrt{n^2(z_2)-n^2(z_1)\sin^2\theta_1}+n(z_2)\right] \\ & - n^2(z_1)|\cos\theta_1| - n^2(z_1)\sin^2\theta_1 \ln[n(z_1)|\cos\theta_1| + n(z_1)]\Big\}. \end{aligned} \tag{12}$$

For the trajectory with $\cos\theta_1$ in the interval $[-\sqrt{1-[n_0/n(z_1)]^2}, 0]$, we have following two cases. (i) If the s given by Eq. (5) is less than $s(z_1, \cos\theta_1, z_r)$, we can still use Eq. (12) to obtain the flight time. (ii) If the s given by Eq. (5) is greater than $s(z_1, \cos\theta_1, z_r)$, the internal reflection happens and the flight time is expressed as

$$t_{f>}(z_1,\cos\theta_1,z_2) = t_f(z_1,\cos\theta_1,z_r) + t_f(z_2,\cos\theta_2,z_r), \tag{13}$$

where

$$\begin{aligned} t_f(z_i,\cos\theta_i,z_r) = \frac{-L}{2c_0(n_s-n_0)}\{ & n^2(z_r)\ln[n(z_r)] - n^2(z_i)|\cos\theta_i| \\ & - n^2(z_r)\ln[n(z_i)|\cos\theta_i| + n(z_i)]\} \end{aligned} \tag{14}$$

with $i = 1$ or 2.

Every bundle is traced until it is absorbed by the medium, escapes from the boundaries of the medium or the total dimensionless flight time is over a very large value, said 100. The dimensionless time is defined by $t^* = c_0\beta t/n_0$.

The slab reflected and transmitted rates of radiation and the absorbed rate inside the medium can be obtained by the present Monte Carlo simulation. The energy of bundles absorbed by the medium or escaping from the boundaries is deposited as E_j, where E_j is the energy leaving the medium or absorbed by the medium in the time interval $[(j-1)\Delta t^*, j\Delta t^*]$ with j denoting a natural number and Δt^* denoting a small time increment. The slab reflected and transmitted rates of radiation are of chief interest in the investigation of short-pulse radiation transport through a planar participating medium. The slab reflected and transmitted rate is calculated as the energy of bundles leaving the medium at the boundary at $z = 0$ and $z = L$, respectively, per unit time. The time-resolved reflectance (R) and transmittance (T) considered in the following sections are defined as the slab reflected and transmitted rate, respectively, normalized by the incident power.

3. Results and discussion

The results of Monte Carlo simulation are considered according to the comparison with those obtained by the discrete ordinates method [17] and the effects of various parameters as follows: bundle number, optical thickness, albedo, refractive index and anisotropically scattering. The optical thickness is defined as $\tau_L = \beta L$ and the albedo (ω) is the ratio of the scattering coefficient and the extinction coefficient. A pulse irradiation with $t_c^* = 1.2$ *and* $t_p^* = 0.4$ is considered here.

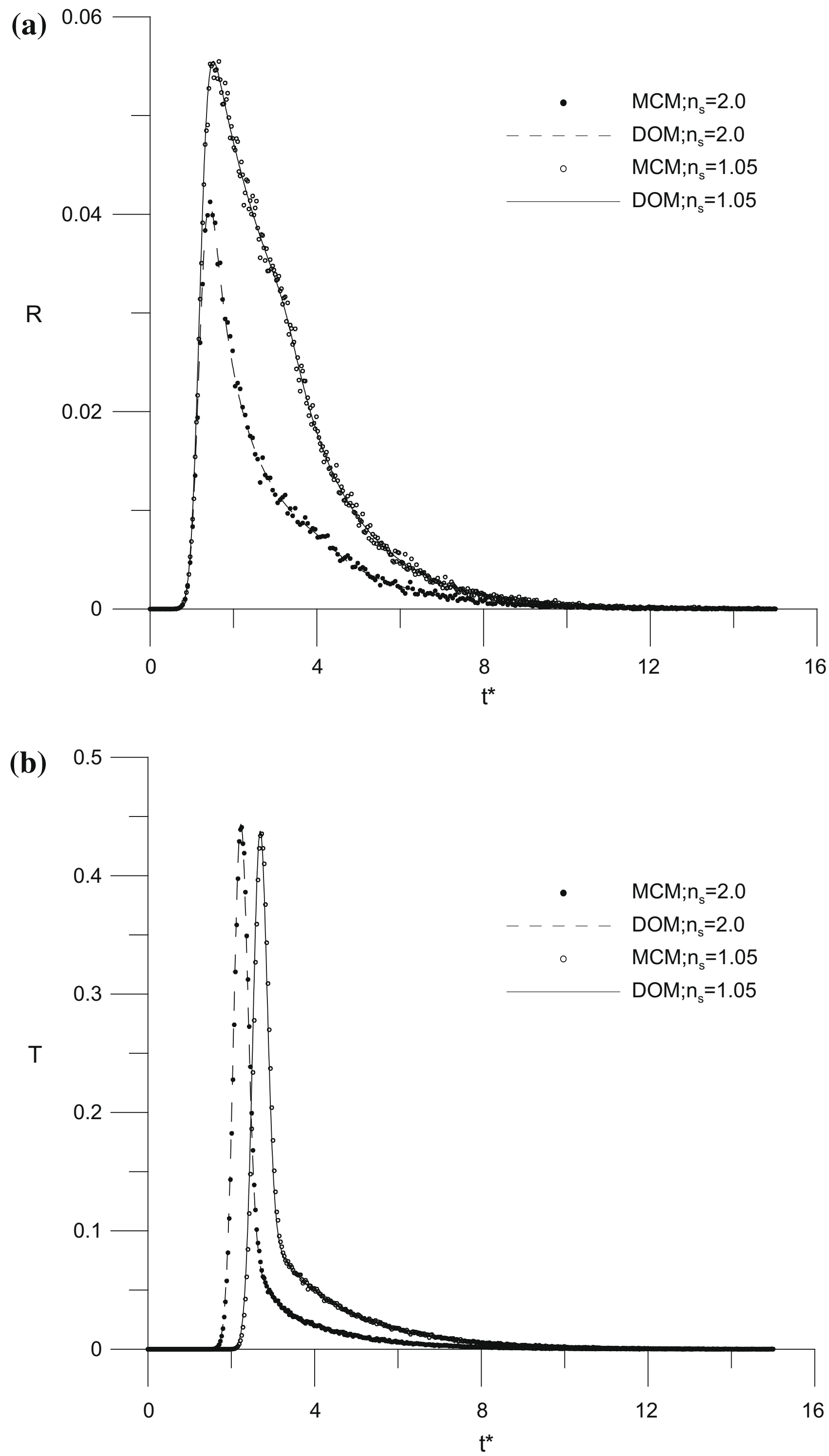

Fig. 2. Comparison of the results obtained by the Monte Carlo method (MCM) and the discrete ordinates method (DOM) [17] for the cases with $\tau_L = 1.0$, $\omega = 1.0$, $a_1 = 0.0$, $n_s = 1.05$ and $n_s = 2.0$: (a) time-resolved reflectance; (b) time-resolved transmittance.

First, we simulate transient radiative transfer in a refractive slab and compare the present results with those obtained by the discrete ordinates method [17]. The time-resolved reflectance and transmittance for optical thicknesses, $\tau_L = 1.0$ and $\tau_L = 15.0$, are presented in Figs. 2 and 3, respectively. There is a very satisfying correspondence between the present results and the discrete ordinates solutions [17].

While 2×10^6 bundles are used to obtain results shown in Fig. 2 for a medium with $\tau_L = 1.0$, the number of bundles for the case with $\tau_L = 15.0$ shown in Fig. 3 is 10^9 in order to simulate the transmittance of very small values. The numerical uncertainty of reflectance and transmittance vs the number of launched photon bundles is examined in Figs. 4 and 5 for three selected bundle numbers: 10^6, 10^7, and 10^8. The magnitude of uncertainty

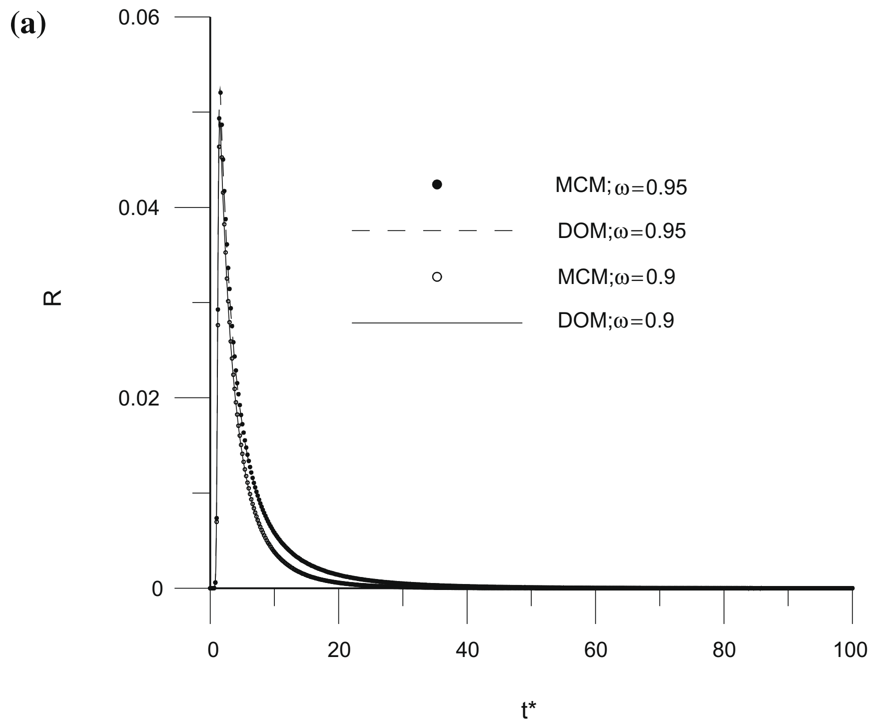

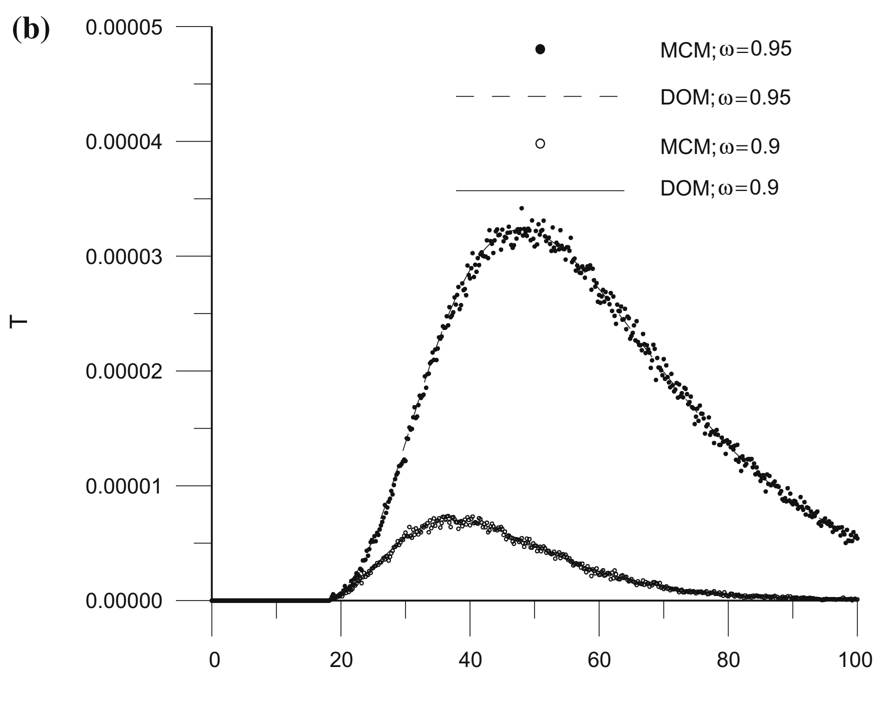

Fig. 3. Comparison of the results obtained by the Monte Carlo method (MCM) and the discrete ordinates method (DOM) [17] for the cases with $\tau_L = 15.0$, $a_1 = 0.0$, $n_s = 1.333$, $\omega = 0.9$ and $\omega = 0.95$: (a) time-resolved reflectance; (b) time-resolved transmittance.

decreases with the increase of bundles. Comparison of Figs. 4 and 5 reveals that the uncertainty of reflectance and transmittance for a medium with an almost constant refractive index is less than that for a medium with a larger gradient of refractive index.

Consider Figs. 2 and 3 again. Fig. 2(a) shows that the reflectance curve has a steep descent following the gradual descent after the peak. The beginning of the steep descent occurs at about the time it takes for the peak of the pulse to travel back and forth between the two boundaries. The change from the gradual descent to the steep descent becomes less obvious as the refractive index increases or the optical thickness increases, as shown in Figs. 2(a) and 3(a). This is because the influence of the boundary at $z = 0$ decreases with the increase of the n_s or the increase of τ_L. The comparison of Figs. 2(a) and 3(a) show that the reflectance increases and its numerical uncertainty decreases with the increase of τ_L. The transmittance has a peak mainly due to reduced collimated pulse

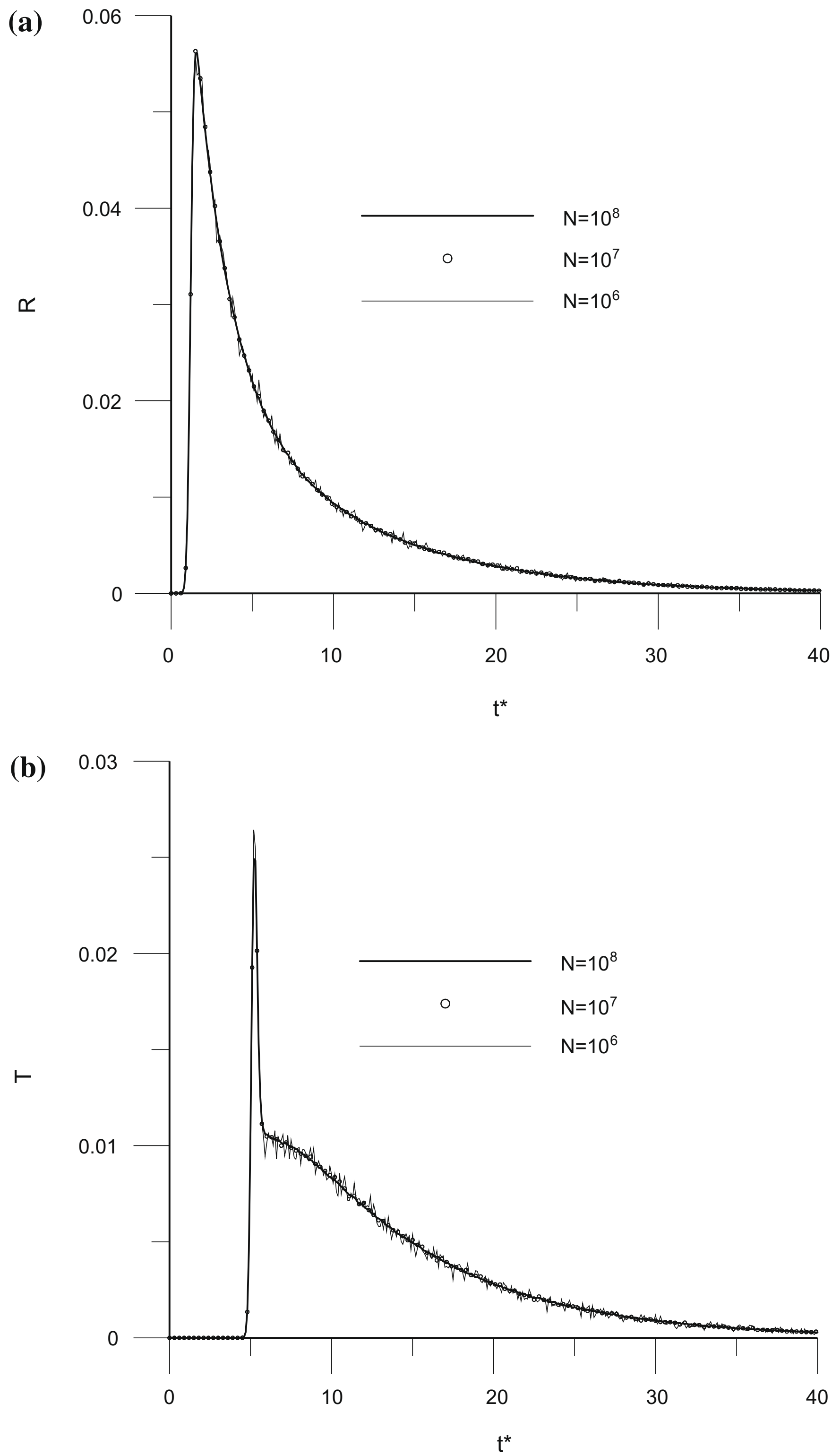

Fig. 4. Influence of the bundle number on numerical uncertainty for the case with $\tau_L = 4.0$, $\omega = 1.0$, $a_1 = 0.0$, $n_s = 1.001$: (a) time-resolved reflectance; (b) time-resolved transmittance.

irradiation and a plump tail due to the scattered radiation, as shown in Fig. 2(b). The plump tail due to the scattered radiation may be dominant and has a local maximum for a medium with large τ_L and ω, as shown in Fig. 3(b). The influence of the albedo on the plump tail of the transmittance curve due to scattering is greater than that on the peak due to reduced pulse irradiation. The influence of the albedo on the transmittance is very strong for a medium with a large optical thickness, as shown in Fig. 3(b). The comparison of Figs. 2(b) and 3(b) show that the transmittance decreases and its numerical uncertainty increases with the increase of τ_L.

Next, let us further examine the effect of the distribution of refractive index. Consider the reflectance curves shown in Fig. 2(a) and the comparison of Figs. 4(a) and 5(a). The slab reflected radiation at $z = 0$ is the result of back-scattering radiation. Thus, in

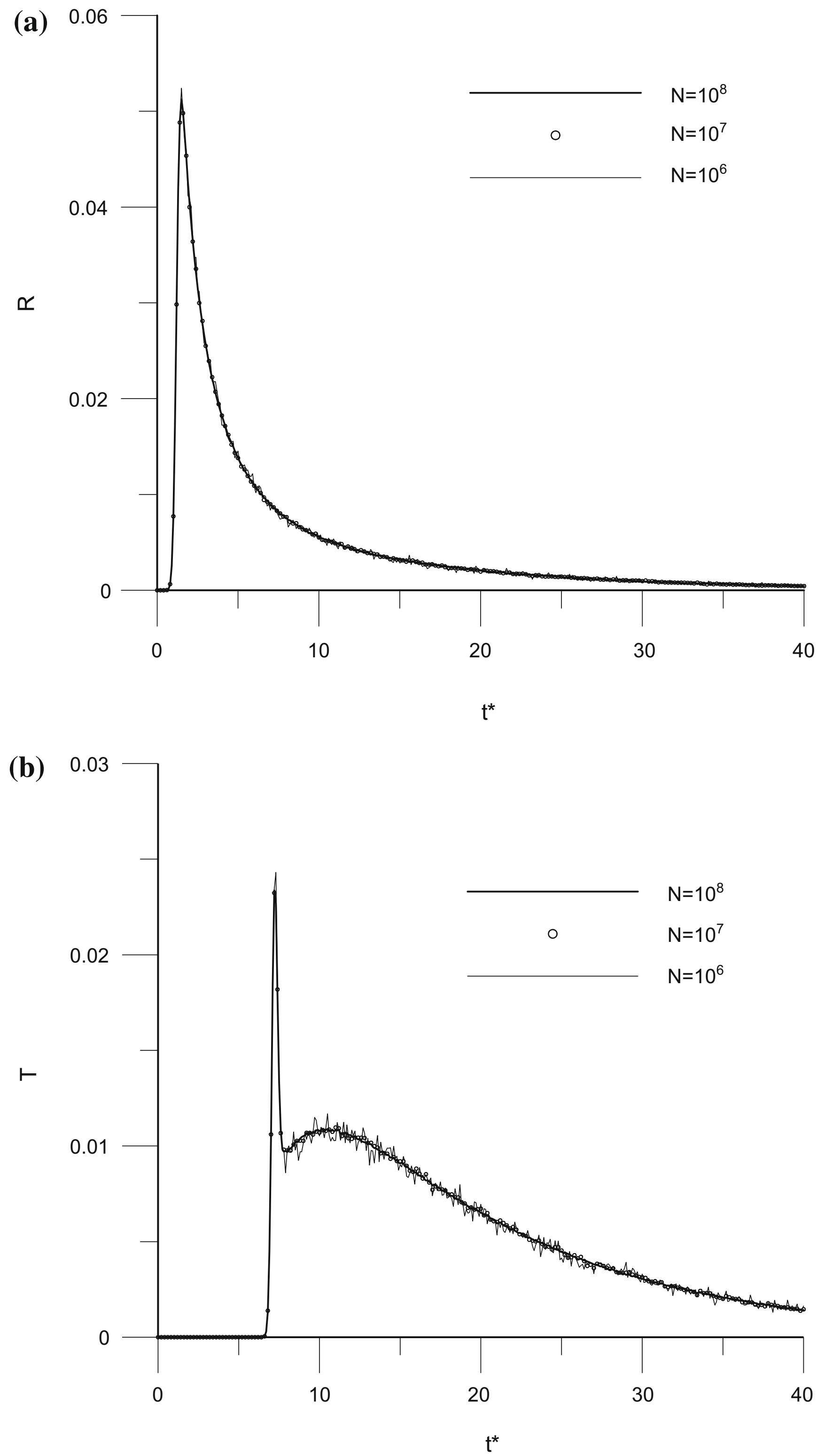

Fig. 5. Influence of the bundle number on numerical uncertainty for the case with $\tau_L = 4.0$, $\omega = 1.0$, $a_1 = 0.0$, $n_s = 2.0$: (a) time-resolved reflectance; (b) time-resolved transmittance.

the present cases with a positive gradient of refractive index a part of the back-scattered radiation cannot reach the boundary at $z = 0$ because of the internal reflection, and so the reflectance decreases with the increase of the n_s. From the transmittance curves shown in Fig. 2(b), we find that the appearance instant of the transmittance peak postpones as the n_s increases. This is because the propagation speed of radiation decreases with the increase of the refractive index. The comparison of Figs. 4(b) and 5(b) shows the same tendency. Besides, the transmittance curve for the case with the refractive index varying linearly from $n_0 = 1$ to $n_s = 2$ (Fig. 5(b)) have two local maximums, while the transmittance curve of the case with a nearly uniform refractive index (Fig. 4(b)) does not have the second local

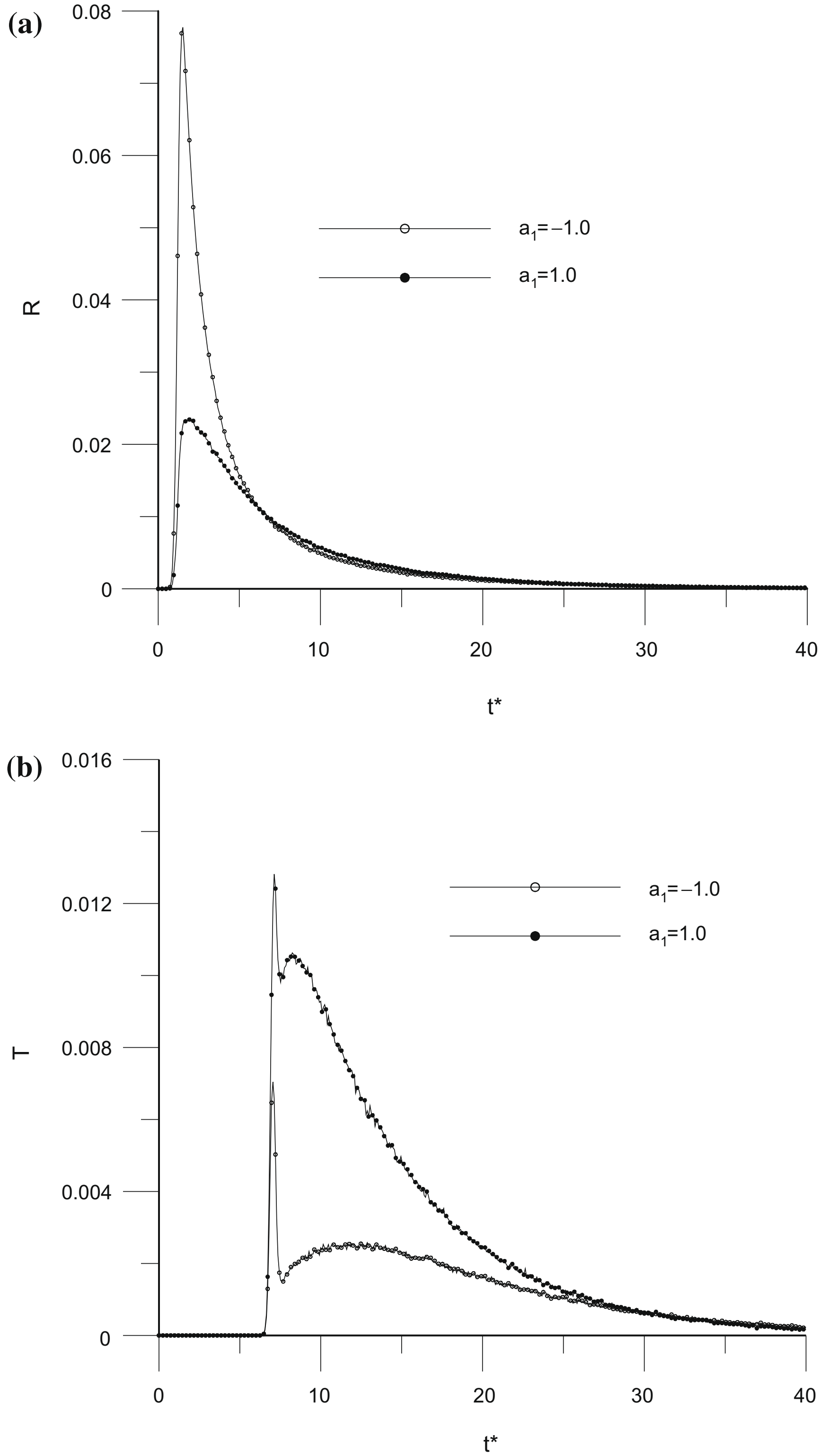

Fig. 6. Effects of anisotropically scattering for the cases with $\tau_L = 5.0$, $\omega = 0.95$, $n_s = 1.333$ $a_1 = 1.0$ and $a_1 = -1.0$: (a) time-resolved reflectance; (b) time-resolved transmittance.

maximum. This is because for a scattering slab with a large gradient of refractive index the curved paths of radiation and the internal reflection of the back-scattered radiation enhances the effect of scattering.

Fig. 6 shows the effects of anisotropically scattering. The time-resolved reflectance decreases with the increase of the anisotropically scattering coefficient for a period of time around the peak of the reflectance curve. Both the peak of the transmittance curve due to reduced collimated pulse irradiation and the maximum of the transmittance curve due to the scattered radiation increase with the increase of the anisotropically scattering coefficient.

4. Concluding remarks

In this work, a Monte Carlo method is developed to simulate transient radiative transfer in a refractive planar medium exposed to a collimated pulse irradiation. The time of flight in closed form is derived for a medium with a linear varying refractive index. The closed-form path length and time of flight are beneficial to the efficiency of the Monte Carlo simulation. The time-resolved reflectance and transmittance of the slab are obtained for various optical thicknesses, scattering albedos, anisotropically scattering coefficients and gradients of refractive index. The present results show a very satisfying correspondence with the discrete ordinates solution [17]. The magnitude of numerical uncertainty decreases with the increase of bundles. To simulate transient radiative transfer in an optically thick medium, we need a large number of bundles. The reflectance increases and its numerical uncertainty decreases with the increase of the τ_L, while the transmittance decreases and its numerical uncertainty increases with the increase of the τ_L. The influence which the continuous variation of refractive index has on transient radiative transfer includes many aspects. The reflectance decreases with the increase of the n_s. The appearance instant of the transmittance peak postpones as the refractive index increases. For a case with a large gradient of refractive index, the curved paths of radiation and the internal reflection of the back-scattered radiation enhances the effect of scattering.

References

[1] P. Ben Abdallah, V. Le Dez, Temperature field inside an absorbing–emitting semi-transparent slab at radiative equilibrium with variable spatial refractive index, J. Quant. Spectrosc. Radiat. Transfer 65 (2000) 595–608.
[2] P. Ben Abdallah, V. Le Dez, Radiative flux field inside an absorbing–emitting semi-transparent slab with variable spatial refractive index at radiative conductive coupling, J. Quant. Spectrosc. Radiat. Transfer 67 (2000) 125–137.
[3] P. Ben Abdallah, V. Le Dez, Thermal emission of a semi-transparent slab with variable spatial refractive index, J. Quant. Spectrosc. Radiat. Transfer 67 (2000) 185–198.
[4] Y. Huang, X.L. Xia, H.P. Tan, Radiative intensity solution and thermal emission analysis of a semitransparent medium layer with a sinusoidal refractive index, J. Quant. Spectrosc. Radiat. Transfer 74 (2002) 217–233.
[5] Y. Huang, X.L. Xia, H.P. Tan, Temperature field of radiative equilibrium in a semitransparent slab with a linear refractive index and gray walls, J. Quant. Spectrosc. Radiat. Transfer 74 (2002) 249–261.
[6] D. Lemonnier, V. Le Dez, Discrete ordinates solution of radiative transfer across a slab with variable refractive index, J. Quant. Spectrosc. Radiat. Transfer 73 (2002) 195–204.
[7] C.C. Chang, C.-Y. Wu, Azimuthally dependent radiative transfer in a slab with variable refractive index, Int. J. Heat Mass Transfer 51 (2008) 2701–2710.
[8] L.H. Liu, H.P. Tan, Q.Z. Yu, Temperature distributions in an absorbing–emitting–scattering semitransparent slab with variable spatial refractive index, Int. J. Heat Mass Transfer 46 (2003) 2917–2920.
[9] Y. Huang, X.G. Liang, X.L. Xia, Monte Carlo simulation of radiative transfer in scattering, emitting, absorbing slab with gradient index, J. Quant. Spectrosc. Radiat. Transfer 92 (2005) 111–120.
[10] L.H. Liu, Benchmark numerical solutions for radiative heat transfer in two-dimensional medium with graded index distribution, J. Quant. Spectrosc. Radiat. Transfer 102 (2006) 293–303.
[11] L.H. Liu, Finite element solution of radiative transfer across a slab with variable spatial refractive index, Int. J. Heat Mass Transfer 48 (2005) 2260–2265.
[12] K.N. Ananda, S.C. Mishra, Discrete transfer method applied to radiative transfer in a variable refractive index semitransparent medium, J. Quant. Spectrosc. Radiat. Transfer 102 (2006) 432–440.
[13] J.M. Zhao, L.H. Liu, Solution of radiative heat transfer in graded index media by least square spectral element method, Int. J. Heat Mass Transfer 50 (2007) 2634–2642.
[14] H.A. Ferwerda, The radiative transfer equation for scattering media with a spatially varying refractive index, J. Opt. A: Pure Appl. Opt. 1 (1999) L1–L2.
[15] J.M. Tualle, E. Tinet, Derivation of the radiative transfer equation for scattering media with a spatially varying refractive index, Opt. Commun. 228 (2003) 33–38.
[16] M. Premaratne, E. Premaratne, A.J. Lowery, The photon transport equation for turbid biological media with spatially varying isotropic refractive index, Opt. Exp. 2 (2005) 389–399.
[17] C.-Y. Wu, Discrete ordinates solution of transient radiative transfer in refractive planar media with pulse irradiation, in: G. de Vahl Davis (Ed.), The Annals of the Assembly for International Heat Transfer, Volume 13, Begell House Inc., Published online, 2006, DOI: 10.1615/IHTC13.p4.120.
[18] L.H. Liu, P.-F. Hsu, Analysis of transient radiative transfer in semitransparent graded index medium, J. Quant. Spectrosc. Radiat. Transfer 105 (2007) 357–376.
[19] M.F. Modest, Radiative Heat Transfer, 2nd ed., Academic Press, San Diego, 2003. Chapter 20.
[20] M.Q. Brewster, Thermal Radiative Transfer and Properties, John Wiley and Sons, New York, 1992. Chapter 14.
[21] S.L. Jacques, Time resolved propagation of ultrashort laser pulses within turbid tissues, Appl. Opt. 28 (1989) 2223–2229.
[22] M.Q. Brewster, Y. Yamada, Optical properties of thick, turbid media from picosecond time-resolved light scattering measurements, Int. J. Heat Mass Transfer 38 (1995) 2569–2581.
[23] C.-Y. Wu, S.-H. Wu, Integral equation formulation for transient radiative transfer in an anisotropically scattering medium, Int. J. Heat Mass Transfer 43 (2000) 2009–2020.
[24] Z. Guo, J. Aber, B.A. Garetz, S. Kumar, Monte Carlo simulation and experiments of pulsed radiative transfer, J. Quant. Spectrosc. Radiat. Transfer 73 (2002) 159–168.